Carbohydrate Polymers 92 (2013) 1633–1640

Contents lists available at SciVerse ScienceDirect

Carbohydrate Polymers

journal homepage: www.elsevier.com/locate/carbpol

Improved stability and controlled release of ω3/ω6 polyunsaturated fatty acids by spring dextrin encapsulation

Jin Xu[b], Wenxiu Zhao[b], Yawei Ning[b], Mohanad Bashari[b], Fengfeng Wu[b], Haiying Chen[b], Na Yang[a,b], Zhengyu Jin[a,b], Baocai Xu[c], Lixia Zhang[d], Xueming Xu[a,b,*]

[a] State Key Laboratory of Food Science and Technology, Jiangnan University, 1800 Lihu AVE, Wuxi 214122, People's Republic of China
[b] School of Food Science and Technology, Jiangnan University, 1800 Lihu AVE, Wuxi 214122, People's Republic of China
[c] State Key Laboratory of Meat Processing and Quality Control, Yurun Group, Nanjing 210041, People's Republic of China
[d] Institute of Farm Products Processing, Jiangsu Academy of Agricultural Sciences, Nanjing Zhongling Street No. 50, Nanjing 210014, Jiangsu, People's Republic of China

ARTICLE INFO

Article history:
Received 20 April 2012
Received in revised form
11 November 2012
Accepted 12 November 2012
Available online 23 November 2012

Keywords:
Spring dextrin
Encapsulation
Poly-unsaturated fatty acid
Molecular dynamic simulation

ABSTRACT

Food grade biopolymers, such as dextrin, have been suggested as a technological solution for the controlled delivery of health promoting substances. The main focus of this work is to improve the stability of poly-unsaturated fatty acids (PUFAs) and controlled release by encapsulating with helical spring dextrin (SD). The encapsulation was formed between SD with a $\overline{DP}$ of 62 and α-linolenic acid (ALA) or linoleic acid (LA) at 60 °C and characterized by WXRD, DSC, TGA and SEM. Under conditions which simulated the human environment of the gastrointestinal system, 21.7% and 18.5% of SD–ALA and SD–LA were released, respectively. A molecular dynamics simulation indicated that the space of helix cavity for ALA–SD complex was larger than that for LA–SD complex. This research work supports the idea that these complexes not only can improve the stability of ALA and LA, but also can achieve the targeted delivery of functional lipids or other bioactive components to the small intestine.

1. Introduction

Poly-unsaturated fatty acids (PUFAs; e.g., omega-3 and omega-6 unsaturated fatty acids) are fatty acids, which contain more than one double bond in their backbone. The omega-3 and omega-6 series PUFAs play a significant role in health promotion and disease prevention by generating potent modulatory molecules for inflammatory responses, including eicosanoids (prostaglandins, and leukotrienes), and cytokines (interleukins) and by affecting the gene expression of various bioactive molecules (Kapoor & Huang, 2006). However PUFAs have low chemical stability during manufacturing, storage and consumption. Besides, PUFAs are also very sensitive to auto-oxidation, generating oxidation products which have a negative effect on the sensory characteristics of the final products.

Encapsulation technology, in which tiny particles or droplets are surrounded by a functional coating, has been developed as an effective approach to controlling flavor, color or preserving properties (Ahmed, Akter, Lee, & Eun, 2010; Wulff, Avgenaki, & Guzmann, 2005; Ziani, Fang, & McClements, 2012). Therefore, this technology is a good alternative to avoiding the auto-oxidation of PUFA by using common, inexpensive and safe food ingredients (Augustin & Hemar, 2009). In this respect, using carbohydrate biopolymers for encapsulation is one of the most effective tools for improving the delivery of functional compounds in foods (Champagne & Fustier, 2007).

In the last 30 years, there was a progressive increase in the number of publications related to cyclodextrins (CDs) (Dick, Rao, Sukumaran, & Lawrence, 1992; Nair & Dismukes, 1983; Panichpakdee & Supaphol, 2011; Trapani et al., 2003) of which α-CD (Bom et al., 2002; Neoh, Yoshii, & Furuta, 2006), β-CD (Arun, Jayaram, Avirah, & Ramaiah, 2011; Choi, Ruktanonchai, Min, Chun, & Soottitantawat, 2010) and γ-CD (Kayaci & Uyar, 2012; Purkayastha, Das, & Syed Jaffer, 2008) are widely used as encapsulation. The inclusion of a guest in a CD cavity consists basically of a substitution of the water molecular by the hydrophobic guest (Astray, Gonzalez-Barreiro, Mejuto, Rial-Otero, & Simal-Gándara, 2009). In recent years, the application of amylose in food-grade delivery system has gained increasing attention due to its biodegradability and availability, which make it a good carbohydrate biopolymer candidate for the development of ingredients of food (Arvisenet, Le Bail, Voilley, & Cayot, 2002; Fanta, Kenar, Byars, Felker, & Shogren, 2010; Jouquand, Ducruet, & Le Bail, 2006). Amylose can include many ligands (e.g. alcohols, aromatic

* Corresponding author at: State Key Laboratory of Food Science and Technology, School of Food Science and Technology, Jiangnan University, 1800 Lihu AVE, Wuxi 214122, People's Republic of China. Tel.: +86 510 85917100; fax: +86 510 85917100.
E-mail address: xmxu@jiangnan.edu.cn (X. Xu).

0144-8617/$ – see front matter © 2012 Elsevier Ltd. All rights reserved.
http://dx.doi.org/10.1016/j.carbpol.2012.11.037

compounds, lipids and emulsifiers) (Yamashita, 1965; Yamashita & Hirai, 1966; Yamashita & Monobe, 1971) with different helical conformations (6_1, 7_1, 8_1 helical conformations) through steric structural change (Conde-Petit, Escher, & Nuessli, 2006; Gelders, Duyck, Goesaert, & Delcour, 2005; Lalush, Bar, Zakaria, Eichler, & Shimoni, 2005). The mechanism by which lipids interact with amylose is that helical amylose has a central hydrophobic cavity in which the hydrocarbon chain of the ligand can reside (Mikus, Hixon, & Rundle, 1946).

In recent years, the V-type crystalline complex has been investigated as a delivery system for bioactive compounds (Lesmes, Cohen, Shener, & Shimoni, 2009; Zabar, Lesmes, Katz, Shimoni, & Bianco-Peled, 2010) because of its resistance to hydrolysis. The hydrolysis of V-type complexes can be regarded as a two-stage process. In the first stage, the amorphous regions, or links of the helices, are readily hydrolyzed (Jane & Robyt, 1984). The second stage, crystalline regions, is slower because the crystalline layers are resistant to amylolysis (Gelders et al., 2005; Heinemann, Zinsli, Renggli, Escher, & Conde-Petit, 2005). Resistance to enzymes (e.g., pancreatic α-amylase) increases with amylose DP and lipid chain length (Gelders et al., 2005). In addition, the hydrolysis rate of the complex in vitro depends on the enzyme activity. For enzymes with low activities, such as enzymes in the oral cavity, only the amorphous material is degraded. In the gastrointestinal tract, however, enzymes are more active and present at higher concentrations than in the oral cavity. These gastrointestinal enzymes can hydrolyze predominantly type I amylose-inclusion complexes to a greater extent (Heinemann et al., 2005). Thus, complexes can be used as a tool for slow release of desired compounds in the gastrointestinal system (Conde-Petit et al., 2006).

Various efforts have made in the development of food-grade delivery systems, which offer the possibility to fabricate products that protect bioactive compounds through processing and storage while controlling and targeting their release in the human gastrointestinal tract (McClements & Li, 2010; Lesmes & McClements, 2009; Velikov & Pelan, 2008). Furthermore the use of simple and low-cost processes and ingredients in the manufacture of such delivery systems has also been of interest (Risch and Reineccius, 1995). 'Spring dextrin' (SD), as we had introduced (Xu et al., 2012), is a linear, poly-disperse saccharide, featuring a repeating (1-4)-α-D-glucose unit. SD is obtained from the hydrolysis of starch with debranching enzymes or amylose with α-amylase, which is low cost. The basic structure of SD is the same as the helical structure of amylose. Since amylose can be used as a food-grade delivery system (Dimantov, Greenberg, Kesselman, & Shimoni, 2004), it follows that SD may also be used as a potential food-grade delivery system.

The objectives of the present study were to: (a) exploit the possibility of using molecular inclusion complex formed by SD as a possible solution for the delivery of PUFA to the consumer; and (b) elucidate the complexes interplay between SD and PUFA by molecular dynamic (MD) simulation in order to extend previous studies on complexation which have not used MD simulation (Gelders et al., 2005; Lesmes et al., 2009).

2. Materials and methods

2.1. Materials

Commercial maize starch was obtained from the local market (Wuxi, China) and stored at 50% relative humidity (Derycke et al., 2005; Jovanovich, Zamponi, Lupano, & Anon, 1992) and 23 °C for 48 h before used. Linoleic acid (LA, 18:2 omega-6), α-linolenic acid (ALA, 18:3 omega-3), α-amylase from porcine pancreas and pancreatin from porcine pancreas, were purchased from Sigma–Aldrich (Shanghai, China). Methanol, 1-decanol, n-hexane, ammonium thiocyanate, hydrochloric acid, sodium hydroxide, sodium acetate–acetic acid, sodium nitrate, potassium hydroxide, sodium phosphate, sodium dihydrogen, phosphate, 1-butanol, isoamyl alcohol and dehydratedalcohol were obtained from China National Medicines Corp., Ltd. (Shanghai, China).

2.2. Preparation of spring dextrin

Amylose was purified as previously described (Takeda, Hizukuri, & Juliano, 1986). The purified amylose was hydrolyzed with α-amylase and the molecular weight was controlled by the duration of hydrolysis. The $\overline{DP}$ of SD was determined by the size-exclusion high-performance liquid chromatography (SE-HPLC). The SD (0.1 g) was dissolved in NaOH (0.5 mol/L, 2 mL) and diluted to 100 mL before incubation at 45 °C for 2 h. The solution was subsequently filtered with a 0.22-μm filter, and a volume of 10 μL (w/w, 0.1%) was injected into the HPLC system for analysis. The HPLC system comprised of a Waters 2410 pump equipped with auto-sampler and differential refractive index detector (Waters, Model 410, Milford, MA, USA). An ultrahydrogel linear column (7.8 mm × 300 mm, Waters) was used, and the column temperature was maintained at 37 °C. The mobile phase was sodium acetate–acetic acid buffer (0.05 mol/L, pH 5.0) containing sodium nitrate (w/w, 0.02%) and the flow rate was 0.9 mL/min.

2.3. Preparation of SD–PUFA complexes

SD (300 mg) was dissolved in 20 mL of preheated (90 °C) KOH (0.1 mol/L), then cooled to 60 °C and pH was maintained at 4.7 under gentle stirring, using 2.0 mol/L HCL. ALA or LA was subsequently added, and the resulting suspensions were kept in a water bath shaker at 60 °C to allow complexation under gentle stirring for 24 h. The complexes were separated from the suspensions by centrifugation (2000 × *g*, 20 min) and the wet pellet was washed using a mixture of ethanol and water (v/v, 50%). The complex was then lyophilized (Labconco Corp., USA) for 24 h (cold-trap temperature −50 °C). The yield of the complex was calculated according to the following formula:

$$\text{yield } (\%) = \frac{(\text{complex, mg})}{[(\text{SD, mg}) + (\text{PUFA, mg})]} \times 100. \quad (1)$$

2.4. WXRD, DSC and TGA – molecular level investigations

XRD patterns were obtained using a Bruker D8-Advance XRD instrument (Bruker AXS Inc., Germany). The samples (0.8 g) were pressed into a pellet (10 mm × 25 mm). The diffractograms were collected under the conditions of 40 kV and 30 mA, with the scanning angle 2θ from 3° to 30° at a scanning rate of 0.6°/min.

The thermal properties of the complexes were analyzed using a Perkin-Elmer Pyris 1 DSC instrument (Perkin-Elmer Inc., USA). A sample (2.0 mg) was added to 6.0 μL of distilled water and sealed in aluminum pans. After equilibration overnight, the solution was scanned from 30 to 130 °C in the calorimeter at 10 °C/min.

Thermogravimetric analysis was conducted with a Mettler Toledo TGA/SDTA851E (Mettler Toledo Corp., Zurich, Switzerland) and STAR software (version 9.01) was used to analyze the thermal stability of the complexes. The operations were performed from 50° to 400 °C at 10 °C/min under nitrogen. A sample mass of 2 mg was maintained throughout the test.

2.5. Microscopic level investigation using SEM

The microscopic complexes were examined by SEM. SEM micrographs were obtained using a JEOL SEM (5400 model) from dry powders plated with gold at an acceleration voltage of 15 kV.

2.6. Oxidative stability tests

The oxidative stability was evaluated by measuring peroxide values (POVs) after the SD–ALA and SD–LA had been stored at 60 °C for different time according to ISO method (ISO 3976). Briefly, LA or ALA was dissolved in methanol/1-decanol/n-hexane (3:1:2, v/v/v, 9.6 mL) solution, ammonium thiocyanate solution (300 mg/mL, 0.05 mL) and iron (II) chloride solution (3 mg/mL, 0.05 mL). The absorption was measured using a 722 grating spectrophotometer (Shanghai Precision and Scientific Instrument Corp., Shanghai, China) at 500 nm after at 10 min hold at room temperature. To make a standard curve for quantitative analysis, a series of iron standard solution was measured using the before mentioned method without the addition of ferrous chloride solution. The peroxide value of the fat, POV, was expressed as millimoles of oxygen per kilogram, by using the following equation:

$$\mathrm{POV} = \frac{m_c - m_{c_0}}{m \times 55.84 \times 2} \quad (2)$$

where m_c and m_{c_0} are the iron weight (μg) of the test sample and sample blank on the iron standard curve, respectively; m is the weight (g) of LA or ALA in the test sample; the atomic weight of iron is 55.84. The iron standard solution (1 g/mL) was prepared by first dissolving reduced iron powder in hydrochloric acid, and then diluted to obtain a series of solutions containing 5 μg, 10 μg, 15 μg and 20 μg of Fe^{3+}, respectively, using methanol/1-decanol/n-hexane (3:1:2, v/v/v) solution. It was worth noticing that, the POV of the LA or ALA in the complex was determined after ultrasonic extraction using methanol/1-decanol/n-hexane (3:1:2, v/v/v) solution as solvent.

2.7. Enzymatic digestion-release analysis

2.7.1. Stability in simulated stomach conditions

The complexes (15 mg) were incubated with 1 mL of HCl (pH 1.5) for 2 h at 37 °C under continuous stirring (15 rpm). The extents of ALA and LA release following the incubation under acidic conditions were measured by extracting the reaction medium with hexane (6 mL), and followed by gas chromatography (GC) analysis. Stability of samples was studied in triplicate. A GC (GC-2010, Shimadzu, Japan) equipped with a fused-silica capillary column (PEG-20M, 30 m × 0.32 mm × 0.25 μm). The temperature programming was 120 °C for 1 min, then ramped at 10 °C/min to 250 °C, and maintained for 2 min. Inlet and detector temperatures were 250 °C. The nitrogen carrier gas flow rate was 2.4 mL/min, hydrogen flow rate to the detector was 25 mL/min, airflow rate was 400 mL/min, and the flow rate of nitrogen makeup gas was 45 mL/min.

2.7.2. Digestion-release in simulated intestinal conditions

The release of ALA and LA from the complex samples was determined through hydrolyzing the samples under simulated gastrointestinal conditions according to the previous methods (Lesmes et al., 2009). A total of 20 mg of each powdered sample was suspended in 2 mL of PBS pancreatin solution and allowed to digest at 37 °C for 0, 6 and 24 h. The amount of ALA and LA in the residual hydrolysate was measured after extraction with hexane, followed by GC quantitative analysis. The digestion-release of samples was studied in triplicate. The release was quantified as follows:

$$\text{release percentage} = \frac{\text{weight of the released PUFA}}{\text{weight of the PUFA in the corresponding complex}} \times 100\% \quad (3)$$

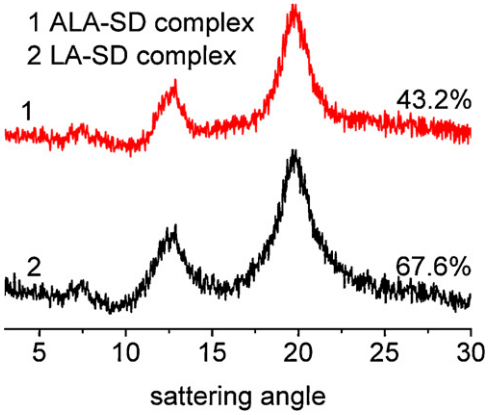

Fig. 1. XRD curves of SD complexed with PUFA: (a) ALA and (b) LA. Degree of crystallization is indicated on the curve.

2.8. Molecular dynamics (MD) simulation

Molecular modeling is a convenient technique to predict the behavior of polymers in solution. The interactions of two enantiomers of PUFA with SD were simulated using the MD module of the HYPERCHEM 8.0 software (Hypercube Inc., Waterloo, Canada). The simulation was performed in a periodic box (30 Å × 30 Å × 50 Å). All established models were energetically pre-optimized and obtained using the Amber force field. The pre-optimized configurations were heat to 333.15 K (60 °C) for 6 ps and then simulate at 333.15 K for 10 ps at a step size of 0.0005 ps. The pre-optimized configurations were equilibrated at this temperature, and then information on the equilibrium conformation was calculated.

3. Results and discussion

3.1. Preparation of complex

The chain length has an effect on the encapsulation efficiency as previously reported (Gelders, Vanderstukken, Goesaert, & Delcour, 2004). In order to achieve complexes, the isolated amylose was hydrolyzed for 1 h with 1 U to control molecular weights. The $\overline{DP}$ value of the SD prepared under the hydrolysis media was 62. From previous literature, if the chain is too long, the conformation would be disordered, resulting in faults in the crystal structure (Gelders et al., 2004). Godet, Bizot, and Buléon (1995) also stated that an amylose chain of DP 20 was too short to complex with a lipid. Therefore, amylose hydrolysis was specifically controlled in the present study. To compare the complexation efficiency of the two complexes, their yields have been measured. Compared with the SD–ALA complex, the yield of the SD–LA complex (58.3%) was higher. The lower yield of the SD–ALA complex (45.8%) might be caused by the three double bonds in ALA that was likely a steric hindrance (Nuessli, Sigg, Conde-Petit, & Escher, 1997). In previous study, it was observed that cis-unsaturated fatty acids complex poorly with amylose, giving low yields compared to fully saturated fatty acids (Eliasson & Krog, 1985).

3.2. Characterization of complexes – WXRD, DSC and TGA

The formation of a V-type complex was verified by measuring the X-ray diffraction of fine white powders obtained by centrifugation and lyophilization of prepared solutions and comparing them to those determined in previous studies (Lalush et al., 2005; Le Bail, Rondeau, & Buléon, 2005). The diffractograms (Fig. 1) confirmed the formation of V-type (type I) structures as inferred from the three

Table 1
Melting temperatures and enthalpies of DSC.

	T_o (°C)[a]	T_m (°C)[a]	ΔH (J/g)[a]
SD–ALA	83.2 ± 0.7	91.7 ± 0.8	12.7 ± 1.7
SD–LA	85.7 ± 0.9	93.4 ± 0.5	14.3 ± 2.6

[a] Data presented as the average standard deviation of three replicates.

broad reflections at 7.5°, 13° and 20°. The degree of crystallinity of SD–ALA was 43.2%, lower than that of SD–LA (67.6%). A similar result was obtained by Zabar, Lesmes, Katz, Shimoni, and Bianco-Peled (2009), who reported that the increase of unsaturation was unfavorable for the formation of amylose inclusion complexes.

The thermal behaviors of the complexes were studied using DSC. The data on DSC of the complexes are presented in Table 1. The melting enthalpies were 14.3 J/g for SD–LA and 12.7 J/g for SD–ALA, which were in agreement with previous reports (Gelders, Goesaert, & Delcour, 2006; Zabar et al., 2010). Notably, the melting enthalpy of the LA complex was higher than that of the ALA complex, suggesting that, the LA complex had a higher degree of crystallinity, as can be seen in the WXRD results. A lower dissociation temperature of the resulting complex was associated with a higher level of unsaturation of the lipid complexed with the SD. This trend is the same as that obtained by Putseys, Derde, Lamberts, Goesaert, and Delcour (2009). Thereby, the number of double bonds in the aliphatic lipid chain has a distinct influence on the thermal properties of the complexes (Karkalas, Ma, Morrison, & Pethrick, 1995; Zabar et al., 2009).

Thermogravimetric analysis was used to study the decomposition pattern and the thermal stability of both the SD and the complexes. As can be seen in Fig. 2, the temperatures, at which initial weight loss (T_i) of ALA, LA, SD, SD–ALA and SD–LA complexes, were 141.2, 151.5, 267.3, 182.9 and 196.3 °C, respectively. The TGA results showed the differences in the thermal stability of the different samples. Thermogravimetric curves of SD–ALA and SD–LA complex indicating that, the complexes were completely decomposed as one unified structure, because one steep step of weight loss has been observed. These phenomena could be explained as described by Yang, Gu, and Zhang (2009); namely that one-step thermogravimetric curve of the amylose-conjugated linoleic acid complex (T_i 240.6 °C) has been observed. The thermogravimetric curves of SD–PUFA were similar to that of the amylose-conjugated linoleic acid complex, since the basic structure of SD is the same as the helical structure of amylose. Differences in T_i between amylose-conjugated linoleic acid and SD–ALA/SD–LA could be explained on the basis of the chain length. Gelders et al. (2005) reported that the dissociation temperature (T_p) of $\overline{DP}$ 60 was lower than that of $\overline{DP}$ 950 when different chain length amylose embedded glyceryl monostearate at 60 °C.

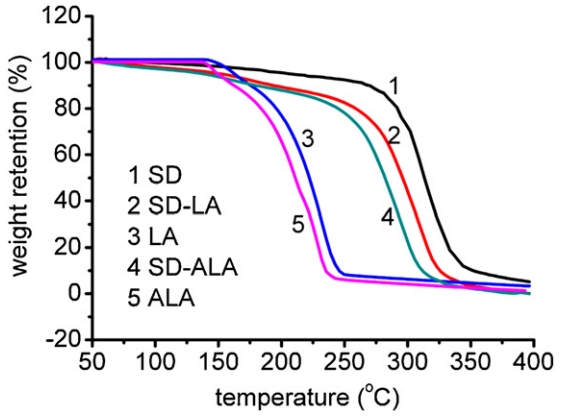

Fig. 2. Thermogravimetric curves of ALA, LA, SD, SD–ALA and SD–LA complexes.

3.3. Microscopic investigation – SEM

SEM images of complexes hosting both fatty acids were examined to study the microscopic attributes of the complexes. The representative micrographs taken from samples produced at 60 °C are shown in Fig. 3(a and b). Comparing SD–ALA and SD–LA, SD–ALA appeared to be smaller, but with no distinct microscopic features, and both of them had a lamellar structure. The complex hydrolyzed with α-amylase in 1 h with 10 U as illustrated in Fig. 3(c and d). Hydrolysis led to the formation of a porous structure, with pores measuring approximately 1 μm in diameter. This phenomenon was attributed to the amorphous regions that were easily hydrolyzed (Heinemann et al., 2005).

3.4. Analysis of oxidative stability of complexes and enzymatic digestion tests

It was reported that the oxidative stability of lipid can be improved by inclusion with starch due to the limitation of oxygen accessibility (Morrison, 1978). Gökmen et al. (2011) recently also showed a reduction of flax seed oil oxidation during bread baking as a result of added V-amylose. Therefore, analysis of oxidative stability was designed to verify the effect of complexation on the oxidation stability of PUFA. The results of oxidative stability tests are presented in Fig. 4a. After appropriate storage times (12 h, 24 h, 48 h and 72 h) at 60 °C, the POVs of ALA and LA extracted from complexes were almost unchanged, while, the POVs of the both controls increased rapidly, suggesting that, the complexes could improve stability of ALA or LA. These results were in good agreement with other studies using amylose as embedding material (Lalush et al., 2005; Yang et al., 2009). Therefore, not only amylose but also SD can improve oxidative stability of PUFA. All of these results indicating that, the inclusion of PUFA by SD can decrease the PUFA oxidation due to the inhibition of oxygen accessibility (Morrison, 1978).

In this part of the study, the protection afforded by complexation to ALA and LA from release in the stomach were tested by incubating SD–ALA and SD–LA complexes in simulated stomach conditions (pH 1.5, 2 h, 37 °C). The results are presented in Fig. 4b. The extent of PUFA release correlated well with their double bonds; i.e., as the number of double bonds increased, the release percentage increased. The effect of the number of double bonds on the release percentage could be explained by the stereo-structure change with the increasing number of double bonds (a less linear ligand requires a wider helix cavity), as the results of DSC and TGA, indicating that, the SD–LA complex was more stable than SD–ALA complex. Eliasson and Krog (1985) also found that the resistances of the complexes with respect to hydrolysis decreased with an increased in the degree of unsaturation.

The results of controlled-release experiments are presented in Fig. 4c. Over time, it the SD–ALA complex released its content more rapidly than the SD–LA complex, however, it released much of its content after 24 h. The release percentages increased with an increased in duration of hydrolysis. SD–ALA released 21.7% after hydrolysis for 24 h by pancreatin, whereas SD–LA released 18.5%. The results suggest that the pancreatin hydrolyzed the complexes (Gelders et al., 2005; Lesmes et al., 2009), and also confirm that type I crystallinity complexes can be hydrolyzed (Heinemann et al., 2005).

The basic structure of SD is the same as the helical structure of amylose. Both of them can entirely complex with PUFA, and then form V type crystals. In a previous study, Yang et al. (2009) confirmed that the amylose-conjugated linoleic acid (CLA) complex

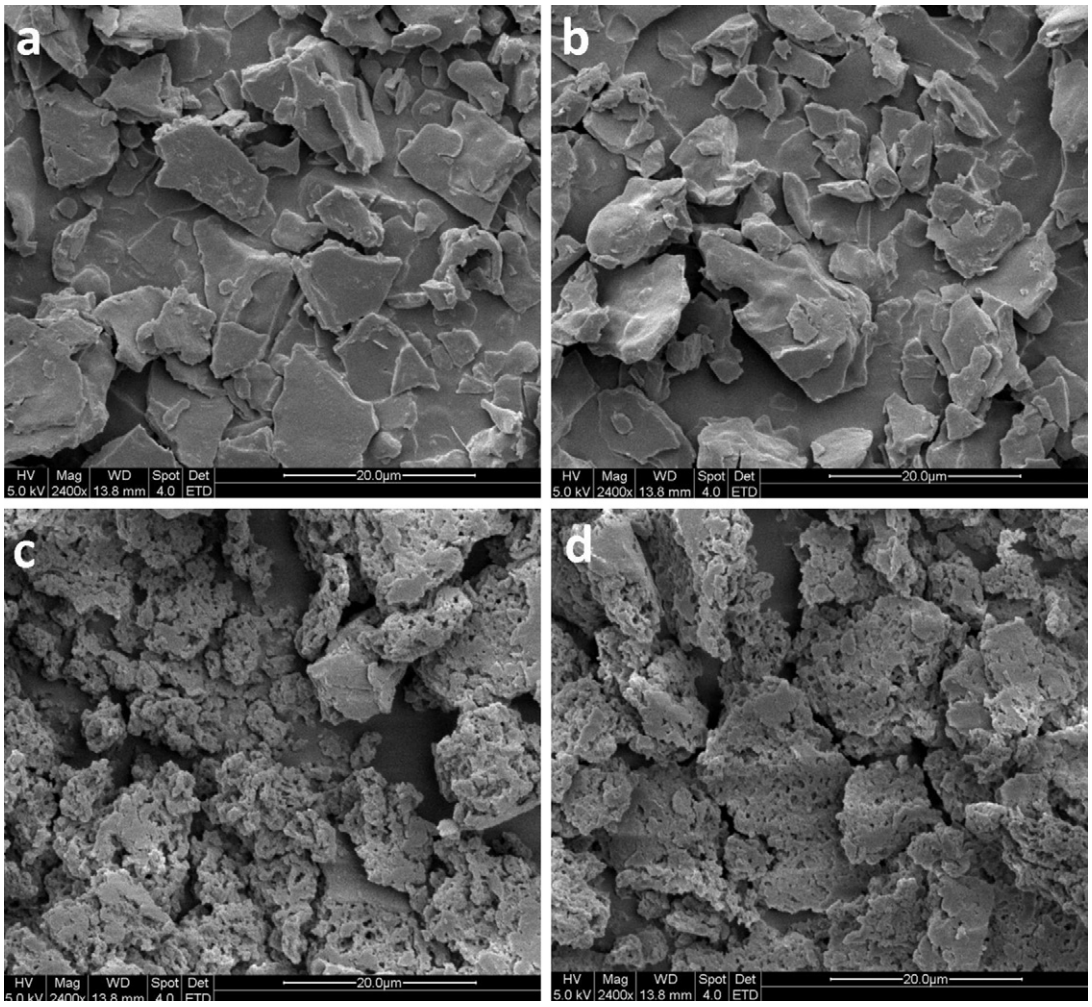

Fig. 3. SEM micrographs of complexes: (a) SD–ALA and (b) SD–LA. SEM micrographs of complexes after hydrolysis: (c) SD–ALA and (d) SD–LA.

can serve as a better vehicle for CLA delivery than the β-CD–CLA complex. This is because of the acid instability (stomach condition), the poor solubility and inherent resistance to enzyme action (small intestine condition) of β-CD–CLA.

3.5. MD simulation analysis

MD simulation is widely used as a theoretical tool to study molecular system at an atomic resolution (Chang & Violi, 2006; Lopez et al., 2009), and can provide a detailed description of dynamic behavior of a system to understand the structure and dynamic of interest. WXRD and DSC confirmed the successful formation of V-type complexes. To understand the mechanism in the self-assembly process, MD was used to examine the phenomenon. The present study monitored the potential energy to get the information on the dynamic configurational equilibrium (Tian et al., 2009) of SD–LA and SD–ALA. It should be noted that the potential energy for the simulative systems at a constant temperature (60 °C, after 10 ps) provided a reasonable description of the system in a dynamic configurational equilibrium. Stable conformations were obtained at 333.15 K (60 °C) after 16-ps MD simulation, according to the stable levels of total energy, potential energy, and the simulation temperature finally has been achieved. The curves of these parameters during the simulation SD–LA complex at 333.15 K in 16 ps are shown in Fig. 5a. The optimized conformation reached equilibrium after approximately 8 ps at 60 °C (Fig. 6a). The

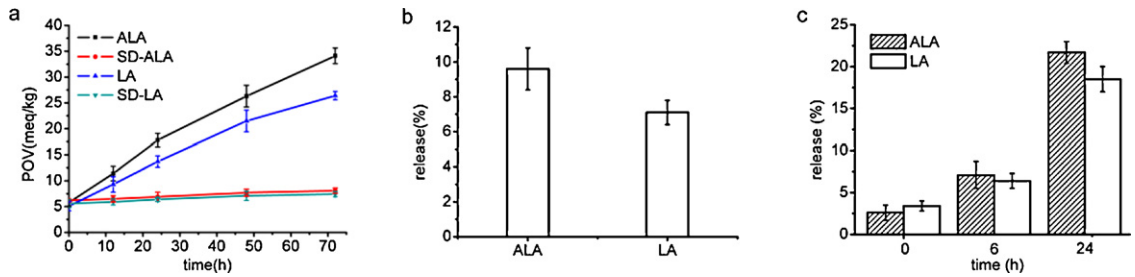

Fig. 4. (a) POV changes in ALA and LA with incubation time at 60 °C. ALA control is free ALA and LA used in complex preparation. (b) Amount of ALA and LA released in simulated stomach conditions (pH 1.5, 2 h at 37 °C). (c) Enzymatically induced release of ALA and LA from V-type crystalline structures.

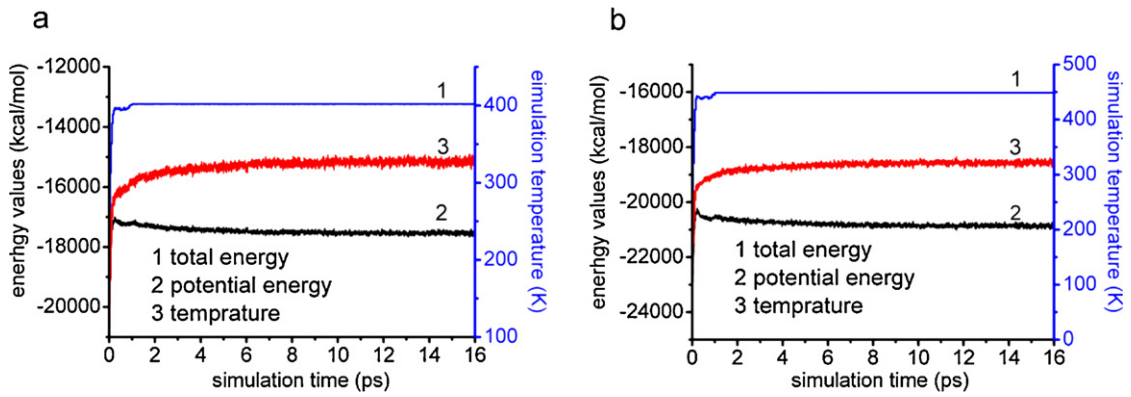

Fig. 5. (a) Curves of total energy, potential energy, and simulation temperature during a simulation performed at 333.15 K in 16 ps (LA) and (b) curves of total energy, potential energy, and simulation temperature during the simulation performed at 333.15 K in 16 ps (ALA).

Table 2
Changes of single point energies of SD–LA and SD–ALA.

	ΔE (kcal/mol)	Non-bonded interaction (kcal/mol)[a]		
		ΔE_{HB}	ΔE_{VdW}	ΔE_{EF}
SD–LA	−502.9 ± 4.6	−82.3 ± 0.7	−476.8 ± 2.6	−11.6 ± 0.3
SD–ALA	−453.2 ± 2.4	−69.3 ± 1.1	−401.1 ± 1.8	−11.8 ± 0.5

BI, bonded interaction; VdW, Van der Waals; HB, hydrogen bonds; and EF, electrostatic forces.
[a] Values are means ± standard deviations from three experiments of simulation; symbol '−' before values means that the force is attractive.

corresponding curves of the SD–ALA complex are obtained at 60 °C for 16 ps and the optimized conformation (Fig. 5b) is in equilibrium after approximately 10 ps at 60 °C (Fig. 6b). Karkalas et al. (1995) suggested that the non-linear structure of a lipid with cis double bonds makes insertion into the linear helix cavity more difficult. However, the carbon atoms adjacent to the double bond might be able to rotate freely, leading to a rather linear structure. This finding implies that complexation could still occur, but that a wider helix cavity would be required, consisting of more than the usual six glucose units per turn. Putseys et al. (2009) also suggested that cis-unsaturated lipids have a kink in their lipid chain and are, thus, subject to steric hindrance inside the helix cavity. The MD results for the complexes with LA and ALA acids were in agreement with this view. The MD results have shown that LA–SD complex was composed of seven glucose residues per turn (Fig. 6a), and ALA–SD complex as closely packed helices with eight glucose residues per turn (Fig. 6b). The different energies of the SD–LA and SD–ALA are shown in Table 2. The change in magnitude of the ΔE would be a sign of the driving force toward complexation. The more negative the interaction energy, the more thermodynamically favorable was the complex (Yousef, Zughul, & Badwan, 2007). Notably, the ΔE of the SD–LA was greater than that of SD–ALA which suggesting that, the SD–LA was more stable than the SD–ALA, which is consistent with the results obtained from the DSC and TGA analysises. As shown in Table 2, some of the main non-bonded interaction forces that may cause forming complex were analyzed by means of the final single point calculation of energies. The results showed that the value of $\Delta E_{H\ SD-LA}$ was greater than $\Delta E_{H\ SD-ALA}$ (the symbol '−' in Table 2 represents the force orientation), which confirmed the results of DSC and TGA ($\Delta H_{SD-LA} > \Delta H_{SD-ALA}$, $T_{i\ SD-LA} > T_{i\ SD-ALA}$). It was thus suggested that the hydrogen bond energy caused the formation of SD–PUFA complex. VdW attraction, as another important factor, showed the maximum value. The phenomenon was interpreted as the increase in VdW attraction probably resulting in the formation of complex since this attraction always plays an important role in promoting non-covalent association (Xie & Soh, 2005). Finally, the electrostatic energy was suggested as a minor factor in comparison to the energy of hydrogen bonds. VdW attraction, hence, is the primary driving force toward SD–PUFA complexation.

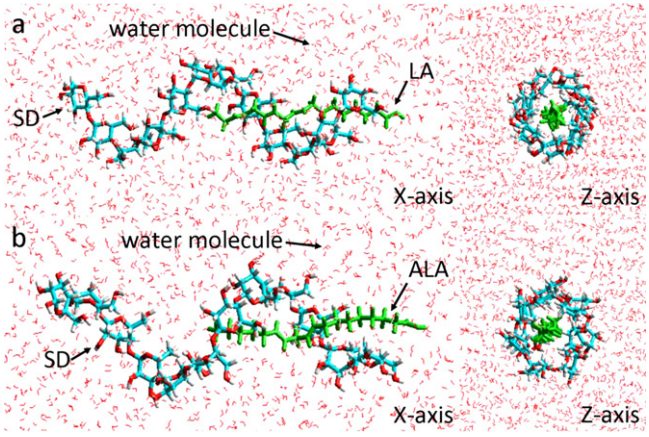

Fig. 6. (a) One of the possible conformations corresponding to interaction of SD and LA at 16 ps and (b) One of the possible conformations corresponding to interaction of SD and ALA at 16 ps.

4. Conclusions

In our current research focus, we proved that SD can complex with ω3/ω6 PUFAs, and verifies the posibility of SD–PUFAs inclusion complexes as a prospective delivery system for PUFAs. The complexes, in turn, protect against oxidation and thermal treatments, which were confirmed by oxidative stability tests, DSC and TGA. Furthermore, the MD simulation indicates that a less linear PUFA requires a wider helix cavity and SD–PUFA interactions were stabilized mainly by van der Waals forces and hydrogen bonds. In addition, controlled release tests showed that SD–PUFAs complexes were not available to gastric digestion, but available under pancreatic conditions to release the included molecule. Thus, SD–PUFA

encapsulation complexes have potential for the delivery of PUFAs to the intestine.

Acknowledgements

This work was supported by National Natural Science Foundation of China (nos. 31071490 and 20976070) and supported by the Fundamental Research Funds for the Central Universities (nos. JUDCF10024 and JUDCF10050).

References

Ahmed, M., Akter, M. S., Lee, J.-C., & Eun, J.-B. (2010). Encapsulation by spray drying of bioactive components, physicochemical and morphological properties from purple sweet potato. *LWT – Food Science and Technology*, *43*, 1307–1312.

Arun, K. T., Jayaram, D. T., Avirah, R. R., & Ramaiah, D. (2011). β-Cyclodextrin as a photosensitizer carrier: effect on photophysical properties and chemical reactivity of squaraine dyes. *The Journal of Physical Chemistry B*, *115*, 7122–7128.

Arvisenet, G., Le Bail, P., Voilley, A., & Cayot, N. (2002). Influence of physicochemical interactions between amylose and aroma compounds on the retention of aroma in food-like matrices. *Journal of Agricultural and Food Chemistry*, *50*, 7088–7093.

Astray, G., Gonzalez-Barreiro, C., Mejuto, J. C., Rial-Otero, R., & Simal-Gándara, J. (2009). A review on the use of cyclodextrins in foods. *Food Hydrocolloids*, *23*, 1631–1640.

Augustin, M. A., & Hemar, Y. (2009). Nano- and micro-structured assemblies for encapsulation of food ingredients. *Chemical Society Reviews*, *38*, 902–912.

Bom, A., Bradley, M., Cameron, K., Clark, J. K., van Egmond, J., Feilden, H., et al. (2002). A novel concept of reversing neuromuscular block: chemical encapsulation of rocuronium bromide by a cyclodextrin-based synthetic host. *Angewandte Chemie*, *114*, 275–280.

Champagne, C. P., & Fustier, P. (2007). Microencapsulation for the improved delivery of bioactive compounds into foods. *Current Opinion in Biotechnology*, *18*, 184–190.

Chang, R., & Violi, A. (2006). Insights into the effect of combustion-generated carbon nanoparticles on biological membranes: a computer simulation study. *The Journal of Physical Chemistry B*, *110*, 5073–5083.

Choi, M.-J., Ruktanonchai, U., Min, S.-G., Chun, J.-Y., & Soottitantawat, A. (2010). Physical characteristics of fish oil encapsulated by β-cyclodextrin using an aggregation method or polycaprolactone using an emulsion–diffusion method. *Food Chemistry*, *119*, 1694–1703.

Conde-Petit, B., Escher, F., & Nuessli, J. (2006). Structural features of starch-flavor complexation in food model systems. *Trends in Food Science & Technology*, *17*, 227–235.

Derycke, V., Vandeputte, G. E., Vermeylen, R., De Man, W., Goderis, B., Koch, M. H. J., et al. (2005). Starch gelatinization and amylose–lipid interactions during rice parboiling investigated by temperature resolved wide angle X-ray scattering and differential scanning calorimetry. *Journal of Cereal Science*, *42*, 334–343.

Dick, D. L., Rao, T. V. S., Sukumaran, D., & Lawrence, D. S. (1992). Molecular encapsulation: cyclodextrin-based analogs of heme-containing proteins. *Journal of the American Chemical Society*, *114*, 2664–2669.

Dimantov, A., Greenberg, M., Kesselman, E., & Shimoni, E. (2004). Study of high amylose corn starch as food grade enteric coating in a microcapsule model system. *Innovative Food Science & Emerging Technologies*, *5*, 93–100.

Eliasson, A. C., & Krog, N. (1985). Physical properties of amylose–monoglyceride complexes. *Journal of Cereal Science*, *3*, 239–248.

Fanta, G. F., Kenar, J. A., Byars, J. A., Felker, F. C., & Shogren, R. L. (2010). Properties of aqueous dispersions of amylose–sodium palmitate complexes prepared by steam jet cooking. *Carbohydrate Polymers*, *81*, 645–651.

Gökmen, V., Mogol, B. A., Lumaga, R. B., Fogliano, V., Kaplun, Z., & Shimoni, E. (2011). Development of functional bread containing nanoencapsulated omega-3 fatty acids. *Journal of Food Engineering*, *105*, 585–591.

Gelders, G. G., Duyck, J. P., Goesaert, H., & Delcour, J. A. (2005). Enzyme and acid resistance of amylose–lipid complexes differing in amylose chain length, lipid and complexation temperature. *Carbohydrate Polymers*, *60*, 379–389.

Gelders, G. G., Goesaert, H., & Delcour, J. A. (2006). Amylose–lipid complexes as controlled lipid release agents during starch gelatinization and pasting. *Journal of Agricultural and Food Chemistry*, *54*, 1493–1499.

Gelders, G. G., Vanderstukken, T. C., Goesaert, H., & Delcour, J. A. (2004). Amylose–lipid complexation: a new fractionation method. *Carbohydrate Polymers*, *56*, 447–458.

Godet, M. C., Bizot, H., & Buléon, A. (1995). Crystallization of amylose–fatty acid complexes prepared with different amylose chain lengths. *Carbohydrate Polymers*, *27*, 47–52.

Heinemann, C., Zinsli, M., Renggli, A., Escher, F., & Conde-Petit, B. (2005). Influence of amylose-flavor complexation on build-up and breakdown of starch structures in aqueous food model systems. *LWT – Food Science and Technology*, *38*, 885–894.

Jane, J.-L., & Robyt, J. F. (1984). Structure studies of amylose-V complexes and retrograded amylose by action of alpha amylases, and a new method for preparing amylodextrins. *Carbohydrate Research*, *132*, 105–118.

Jouquand, C., Ducruet, V., & Le Bail, P. (2006). Formation of amylose complexes with C6-aroma compounds in starch dispersions and its impact on retention. *Food Chemistry*, *96*, 461–470.

Jovanovich, G., Zamponi, R. A., Lupano, C. E., & Anon, M. C. (1992). Effect of water content on the formation and dissociation of the amylose–lipid complex in wheat flour. *Journal of Agricultural and Food Chemistry*, *40*, 1789–1793.

Kapoor, R., & Huang, Y.-S. (2006). Gamma linolenic acid: an antiinflammatory omega-6 fatty acid. *Current Pharmaceutical Biotechnology*, *7*, 531–534.

Karkalas, J., Ma, S., Morrison, W. R., & Pethrick, R. A. (1995). Some factors determining the thermal properties of amylose inclusion complexes with fatty acids. *Carbohydrate Research*, *268*, 233–247.

Kayaci, F., & Uyar, T. (2012). Encapsulation of vanillin/cyclodextrin inclusion complex in electrospun polyvinyl alcohol (PVA) nanowebs: prolonged shelf-life and high temperature stability of vanillin. *Food Chemistry*, *133*, 641–649.

Lalush, I., Bar, H., Zakaria, I., Eichler, S., & Shimoni, E. (2005). Utilization of amylose–lipid complexes as molecular nanocapsules for conjugated linoleic acid. *Biomacromolecules*, *6*, 121–130.

Le Bail, P., Rondeau, C., & Buléon, A. (2005). Structural investigation of amylose complexes with small ligands: helical conformation, crystalline structure and thermostability. *International Journal of Biological Macromolecules*, *35*, 1–7.

Lesmes, U., Cohen, S. H., Shener, Y., & Shimoni, E. (2009). Effects of long chain fatty acid unsaturation on the structure and controlled release properties of amylose complexes. *Food Hydrocolloids*, *23*, 667–675.

Lesmes, U., & McClements, D. J. (2009). Structure–function relationships to guide rational design and fabrication of particulate food delivery systems. *Trends in Food Science & Technology*, *20*, 448–457.

Lopez, C. A., Rzepiela, A. J., de Vries, A. H., Dijkhuizen, L., Hunenberger, P. H., & Marrink, S. J. (2009). Martini coarse-grained force field: extension to carbohydrates. *Journal of Chemical Theory and Computation*, *5*, 3195–3210.

McClements, D. J., & Li, Y. (2010). Structured emulsion-based delivery systems: controlling the digestion and release of lipophilic food components. *Advances in Colloid and Interface Science*, *159*, 213–228.

Mikus, F. F., Hixon, R. M., & Rundle, R. E. (1946). The complexes of fatty acids with amylose. *Journal of the American Chemical Society*, *68*, 1115–1123.

Morrison, W. R. (1978). The stability of wheat starch lipids in untreated and chlorine-treated cake flours. *Journal of the Science of Food and Agriculture*, *29*, 365–371.

Nair, B. U., & Dismukes, G. C. (1983). Models for the photosynthetic water oxidizing enzyme. 1. A binuclear manganese(III)–β-cyclodextrin complex. *Journal of the American Chemical Society*, *105*, 124–125.

Neoh, T.-L., Yoshii, H., & Furuta, T. (2006). Encapsulation and release characteristics of carbon dioxide in α-cyclodextrin. *Journal of Inclusion Phenomena and Macrocyclic Chemistry*, *56*, 125–133.

Nuessli, J., Sigg, B., Conde-Petit, B., & Escher, F. (1997). Characterization of amylose-flavour complexes by DSC and X-ray diffraction. *Food Hydrocolloids*, *11*, 27–34.

Panichpakdee, J., & Supaphol, P. (2011). Use of 2-hydroxypropyl-β-cyclodextrin as adjuvant for enhancing encapsulation and release characteristics of asiaticoside within and from cellulose acetate films. *Carbohydrate Polymers*, *85*, 251–260.

Purkayastha, P., Das, D., & Syed Jaffer, S. (2008). Differential encapsulation of trans-2-[4-(dimethylamino)styryl] benzothiazole in cyclodextrin hosts: application towards nanotubular suprastructure formation. *Journal of Molecular Structure*, *892*, 461–465.

Putseys, J. A., Derde, L. J., Lamberts, L., Goesaert, H., & Delcour, J. A. (2009). Production of tailor made short chain amylose–lipid complexes using varying reaction conditions. *Carbohydrate Polymers*, *78*, 854–861.

Risch, S. J., & Reineccius, G. A. (1995). Encapsulation and controlled release of food ingredients. In G. A. Reineccius (Ed.), *Controlled release techniques in the food industry* (pp. 8–25). Washington, DC: American Chemical Society.

Takeda, Y., Hizukuri, S., & Juliano, B. O. (1986). Purification and structure of amylose from rice starch. *Carbohydrate Research*, *148*, 299–308.

Tian, Y., Li, Y., Manthey, F. A., Xu, X., Jin, Z., & Deng, L. (2009). Influence of β-cyclodextrin on the short-term retrogradation of rice starch. *Food Chemistry*, *116*, 54–58.

Trapani, G., Lopedota, A., Boghetich, G., Latrofa, A., Franco, M., Sanna, E., et al. (2003). Encapsulation and release of the hypnotic agent zolpidem from biodegradable polymer microparticles containing hydroxypropyl-β-cyclodextrin. *International Journal of Pharmaceutics*, *268*, 47–57.

Velikov, K. P., & Pelan, E. (2008). Colloidal delivery systems for micronutrients and nutraceuticals. *Soft Matter*, *4*, 1964–1980.

Wulff, G., Avgenaki, G., & Guzmann, M. S. P. (2005). Molecular encapsulation of flavours as helical inclusion complexes of amylose. *Journal of Cereal Science*, *41*, 239–249.

Xie, Y. H., & Soh, A. K. (2005). Investigation of non-covalent association of single-walled carbon nanotube with amylose by molecular dynamics simulation. *Materials Letters*, *59*, 971–975.

Xu, J., Zhao, W., Ning, Y., Jin, Z., Xu, B., & Xu, X. (2012). Comparative study of spring dextrin impact on amylose retrogradation. *Journal of Agricultural and Food Chemistry*, *60*, 4970–4976.

Yamashita, Y. (1965). Single crystals of amylose V complexes. *Journal of Polymer Science Part A: General Papers*, *3*, 3251–3260.

Yamashita, Y., & Hirai, N. (1966). Single crystals of amylose V complexes. II. Crystals with 7_1 helical configuration. *Journal of Polymer Science Part A-2: Polymer Physics*, *4*, 161–171.

Yamashita, Y., & Monobe, K. (1971). Single crystals of amylose V complexes. III. Crystals with 8_1 helical configuration. *Journal of Polymer Science Part A-2: Polymer Physics*, *9*, 1471–1481.

Yang, Y., Gu, Z., & Zhang, G. (2009). Delivery of bioactive conjugated linoleic acid with self-assembled amylose–CLA complex. *Journal of Agricultural and Food Chemistry*, *57*, 7125–7130.

Yousef, F., Zughul, M., & Badwan, A. (2007). The modes of complexation of benzimidazole with aqueous β-cyclodextrin explored by phase solubility, potentiometric titration, ^{1}H NMR and molecular modeling studies. *Journal of Inclusion Phenomena and Macrocyclic Chemistry*, *57*, 519–523.

Zabar, S., Lesmes, U., Katz, I., Shimoni, E., & Bianco-Peled, H. (2009). Studying different dimensions of amylose-long chain fatty acid complexes: molecular, nano and micro level characteristics. *Food Hydrocolloids*, *23*, 1918–1925.

Zabar, S., Lesmes, U., Katz, I., Shimoni, E., & Bianco-Peled, H. (2010). Structural characterization of amylose-long chain fatty acid complexes produced via the acidification method. *Food Hydrocolloids*, *24*, 347–357.

Ziani, K., Fang, Y., & McClements, D. J. (2012). Encapsulation of functional lipophilic components in surfactant-based colloidal delivery systems: Vitamin E, vitamin D, and lemon oil. *Food Chemistry*, *134*, 1106–1112.